Probabilistic seasonal outlook for the rainy season over India by monitoring the onset dates using GPM IMERG satellite-based precipitation

Jayasankar Chempampadam Balasubramannian[1, 2], and Vasubandhu Misra[1, 2, 3]

[1]Center for Ocean-Atmospheric Prediction Studies, Florida State University, Tallahassee, Florida, USA.

[2]Department of Earth, Ocean and Atmospheric Science, Florida State University, Tallahassee, Florida, USA.

[3]Florida Climate Institute, Florida State University, Tallahassee, Florida, USA.

Corresponding Author (Jayasankar Chempampadam Balasubramannian, cbjayasankar@gmail.com)

Abstract

We utilized the Integrated Multi-Satellite Retrievals for Global Precipitation Mission version 6 (IMERG) rainfall observation (available in real time) over India to determine the onset and withdrawal of the rainy season. The annual mean climatology derived from IMERG observations over India aligned closely with the rain gauge-based India Meteorological Department observation. The IMERG rainfall time series was randomly perturbed to generate 101 ensemble members at every grid point of the rainfall analysis to obtain a corresponding ensemble of the onset and withdrawal dates of the rainy season. The perturbations were designed to sample the uncertainty due to random synoptic or mesoscale rain events influencing the diagnosis of the onset/withdrawal dates at the granularity of the IMERG observations (available at 10 km grid). Following earlier studies, we find from the IMERG dataset that seasons with an earlier onset date are strongly related to a lengthier and wetter season, whereas seasons with a later onset date correspond to a shorter and a drier season. In contrast, the connections between El Niño-Southern Oscillation (ENSO) and Indian Ocean dipole (IOD) with the onset, withdrawal, seasonal length, and rainfall of the rainy season were comparatively weaker over most of India. The generation of ensembles in this study underscores the potential for real-time application of generating reliable, probabilistic seasonal outlooks of the rainy season over India by leveraging the local links amongst onset date, seasonal length, and seasonal rainfall anomalies. This potential is further confirmed by the high probabilistic skill scores of the seasonal outlooks using the area under the relative operating characteristic curve method.

1. Introduction

India's water and agriculture sectors rely heavily on copious summer monsoon rainfall, emphasizing its critical role in defining the country's agrarian economy and water resource management (Gadgil and Gadgil 2006). The seasonal progression of the Indian Summer Monsoon (ISM) season has an impact not only on agricultural yields but also on other sectors such as economy and ecology (Lal 2000). Based on rainfall patterns, wind conditions, and outgoing longwave radiation, the India Meteorological Department (IMD) officially declare the date of monsoon onset over Kerala (MoK) each year. In a normal year, the ISM season begins in southern peninsular India on June 1st (with MoK), spreads throughout the country by mid-July, and then begins to retreat on September 1st (Pai et al. 2020).

There are many different definitions for the monsoon onset; however, it is typically considered as a quick, substantial, and prolonged increase in rainfall after May 10th, accompanied by a persistent change in wind direction to southwesterlies associated with the summer monsoon flow (Pai and Rajeevan 2009). In addition to the rainfall-based definitions (e.g., Ananthakrishnan and Soman 1988; Noska and Misra 2016; Misra et al. 2017b), several other atmospheric dynamical and thermodynamical variables (winds, outgoing longwave radiation, temperature, moisture flux convergence, and precipitable water) were utilized to identify the onset of summer monsoon rainfall (e.g., Fasullo and Webster 2003, Zeng and Lu 2004, Prasad and Hayashi 2005, Joseph et al. 2006, Wang et al. 2009, Walker and Bordoni 2016, Stolbova et al. 2016). These variables provide a comprehensive understanding of the atmospheric conditions and dynamics that influence the onset and total summer monsoon rainfall over India. According to Bombardi et al. (2019), monsoon onset detection methods can be grouped into local-scale and regional-to-large-scale approaches, though the latter often show weak correlation with local observations. All these approaches produce somewhat similar onset dates, but their connections with the local-scale onset of the rainfall during the ISM differ (Moron and Robertson 2014; Noska and Misra 2016; Fitzpatrick et al. 2016).

Owing to variations in the onset and withdrawal date of the monsoon season there are considerable spatial and temporal variations in the availability of the rainwater and length of the rainy season

63 (determined solely based on rain rates) over India (Joseph et al. 1994; Lal 2000; Wang et al. 2002;

64 Misra et al. 2017a; Misra et al. 2018). Preenu et al. (2017) indicate from IMD archive that the

65 earliest onset of the ISM was May 11, 1918, and the most delayed onset of ISM was Jun 18, 1972.

66 Several studies discuss the interannual variability of monsoon onset dates in India and its

67 teleconnection with El Niño and the Southern Oscillation (ENSO) and the Indian Ocean Dipole

68 (IOD, Xavier et al. 2007; Sankar et al. 2010; Misra et al. 2017a; Pradhan et al. 2017; Choudhury

69 et al. 2021). In ENSO and IOD years, the monsoon onset is altered by the modulation of the

70 teleconnections with SST anomalies in the tropical oceans, which affect the Walker and Hadley

71 circulations, respectively (Pradhan et al. 2017). Significant changes in the large-scale atmospheric

72 patterns over the monsoon areas are identified during the onset of the monsoon over India (Joseph

73 et al. 1994). According to Wang et al. (2013), the interannual variations in ocean-atmosphere

74 interaction processes significantly influence the association between the monsoon onset and

75 ENSO, which is driven by the meridional SST gradient across the Indian Ocean. Noska and Misra

76 (2016) show that the variations in the onset and withdrawal date of the rainy season over India that

77 largely overlaps with ISM are linked to the variability of the cross-equatorial upper-ocean heat

78 transport in the Indian Ocean, variations in large-scale atmospheric and oceanic circulations, and

79 regional ocean-atmosphere thermal gradients. In addition, internal variability of ISM arising from

80 intraseasonal oscillations (ISOs), can significantly influence the monsoon rainfall and as well as

81 the onset and withdrawal characteristics of the ISM (Goswami and Ajaya Mohan, 2001; Goswami

82 and Xavier, 2005; Karmakar and Misra 2019). Monsoon ISOs are typically classified into active

83 (above normal) and break (below normal) phases, and the frequency of these phases plays a crucial

84 role in determining the seasonal mean monsoon rainfall (Goswami and Ajaya Mohan, 2001).

85 Karmakar and Misra (2019) found that a majority of local onset dates (59%) occur during the

86 positive developing phases of high-frequency ISOs, while a majority of withdrawal dates (62%)

87 occur during the positive decaying phases of low-frequency ISOs.

88

89 It may be noted that we make a subtle distinction between the ISM and rainy seasons, with the

90 latter solely determined by rain rates which includes pre- and post-monsoon seasonal rainfall (e.

91 g., Noska and Misra 2016) while the former is usually a fixed calendar season (June to September)

92 and coincides additionally with the seasonal cycle of circulation features and other thermodynamic

93 factors. Figure S1 highlights the difference between the rainy season and climatological ISM (June

94   to September), which makes it evident that the rainy season accumulates more rainfall in southern

95   peninsular India and in regions east of the central monsoon region. Similarly, when compared to

96   the ISM season, the rainy season has slightly less total rainfall over both western, northern India,

97   and parts of northeastern India. It may be noted that the definition of the rainy season allows for a

98   variable length compared to the fixed calendar season of, which stems from the former including

99   pre-monsoon rainfall and rainfall from pre-monsoon and post-monsoon rainfall. For instance,

100   tropical cyclones are also included in the rainy season defined here, and they significantly

101   contribute to the annual rainfall in some parts of eastern India. Pre- and post-monsoon tropical

102   cyclones can contribute up to 25% of the yearly rainfall in some parts of India, even though the

103   southwest monsoon is the main component of our defined rainy season (Khouakhi et al. 2017).

104

105   The information about the arrival of the monsoon rainfall is imperative for farmers to plan their

106   strategy for the upcoming season. There are many attempts to predict the MoK; however, it

107   remains a challenge due to the intricate interplay between large-scale atmospheric circulation and

108   localized convective processes, resulting in substantial spatial variability in onset dates (Kung and

109   Shariff 1980; Rajeevan and Dubey 1995; Pai and Rajeevan 2007; Pradhan et al. 2017). Many

110   studies have shown that variations of the MoK have very little influence on the mean rainfall

111   anomalies of the ISM (Dhar et al. 1980; Mooley and Parthasarthy 1984; Mooley and Shukla 1987;

112   Misra and DiNapoli 2014). Furthermore, MoK is known to have insignificant relationship with

113   subsequent progression of the onset isochrones of the ISM (Bansod et al. 1991; Fasullo and

114   Webster 2003; Pai and Rajeevan 2007). Noska and Misra (2016) proposed an objective method to

115   define the onset and withdrawal of the rainy season based on area averaged all India daily rainfall,

116   and they found that mean anomalies of the rainy season are closely linked with variations in the

117   onset and withdrawal dates of the rainy season. In addition, they validated the defined onset and

118   withdrawal of the rainy season for consistency by comparing them with the seasonal evolution of

119   key dynamic and thermodynamic variables associated with the ISM. In a following study, Misra

120   et al. (2018) obtained local onset (withdrawal) dates of the Indian rainy season at the granularity

121   of the rainfall analysis and showed that they are negatively (positively) correlated with rainfall

122   anomalies of the rainy season across the Indian region. These studies suggest that monitoring the

123   local onset date of the rainy season provides a good indication of the evolution of the seasonal

124   length and rainfall of the forthcoming rainy season (i.e., the entire duration of the rainy season at

125   each grid points) and supporting its use in predictability studies. Bhardwaj and Misra (2019) found
126   that Remotely Sensed Rainfall Products such as Tropical Rainfall Measuring Mission (TRMM)
127   Multi-satellite Precipitation Analysis (TMPA) produce local onset and withdrawal dates similar to
128   IMD observations. In comparison to traditionally identified onset of ISM, which are often limited
129   to defining the onset over Kerala (e.g., MoK), the proposed method enables the generation of
130   spatially continuous maps of onset date evolution. By capturing regional heterogeneity, it provides
131   a more nuanced understanding of the spatiotemporal progression of onset of the rainy season
132   across India. This simple rainfall-based definition was found useful for monitoring the onset of the
133   rainy season in real-time and issuing the outlook of the rainy season over various regions such as
134   Florida (Misra et al. 2022), and Central America (Rodgers et al. 2024).

135

136   Many studies have used the IMERG data set as one of their primary dataset for the analysis of the
137   ISM (Bushair et al. 2019; Thakur et al. 2020; Saikrishna et al. 2021; Phadtare et al. 2023). In this
138   study, we employ a rainfall-based objective method to define the local onset and withdrawal of the
139   rainy season, leveraging the high-resolution IMERG dataset available since January 2001. Our
140   approach captures the actual arrival and retreat of persistent rainfall at each grid point by
141   identifying the onset and withdrawal of the rainy season. This approach also accounts for pre- and
142   post-monsoon rainfall, providing a more complete representation of the rainy season—particularly
143   in regions where events such as tropical cyclones contribute significantly to seasonal rainfall totals.
144   In this study, utilizing IMERG's 12-hour latency product, we demonstrate the potential for real-
145   time monitoring of the onset of the rainy season, which aids in anticipating the anomalies of the
146   seasonal length and seasonal accumulated rainfall (hereafter referred to as seasonal rainfall) across
147   India. Motivated from the grid-point level definition of onset and withdrawal dates established by
148   Misra et al. (2018) and Bhardwaj and Misra (2019), this study advances this framework by how
149   the IMERG 12-hour latency product can be effectively used to monitor these parameters at fine
150   spatial scales, enabling better anticipation of anomalies of the seasonal length and seasonal rainfall.
151   In addition, the novelty of this work lies in the use of a perturbation technique applied in the
152   diagnosis of onset/withdrawal dates of the rainy season over India following Misra et al. (2023)
153   and Rodgers et al. (2024) to generate 101 ensembles of daily rainfall data. This approach is the
154   first of its kind over the Indian region and allows us to define an ensemble of local onset and
155   withdrawal dates, aiding in the probabilistic estimate of the evolution of the rainy season that

156 accounts for observational and analysis uncertainties. Hereafter, the term 'onset' refers to local or
157 grid point-specific onset dates of the rainy season.

158

159 Additionally, this study explores the interannual variation of the evolution of the rainy season and
160 its link to large-scale forcing such as ENSO and IOD and compares their viability as predictors of
161 the rainy seasons to the local links we establish with the variations of the onset dates. We believe
162 that the insights from this study will have significant potential applications in agricultural planning
163 and water resource management.

164

2. Data and Methodology

2.1 Data

167 The analysis performed in this study utilized daily precipitation data from the IMERG version 6
168 (Huffman et al. 2019). This dataset is part of the Global Precipitation Measurement (GPM)
169 mission, which was launched in 2014 and is co-operated by NASA and the Japan Aerospace
170 Exploration Agency (JAXA). The 0.1° grid resolution (~10 km) IMERG data are available at half-
171 hourly intervals from June 2000 to the present. The dataset comprises early, late, and final run
172 products, which have latencies of approximately 4 hours (Early), 12 hours (Late), and 3.5 months
173 (Final). The IMERG late run incorporates data from multiple sources, such as satellite microwave
174 and infrared estimations, precipitation gauge analysis, and other potential precipitation estimators.
175 This dataset provides detailed temporal and spatial coverage for both the TRMM and GPM eras
176 worldwide. However, in this study, we used the daily 12-hour latency product (daily averages were
177 estimated from half-hourly products), which has great potential for monitoring the rainy season in
178 real-time. To assess the fidelity of the 12-hour latency product of IMERG over India, we have
179 compared it with the corresponding Final product of IMERG and also used rain gauge-based IMD
180 gridded rainfall data for the period 2001 - 2023 at 0.25° × 0.25° resolution (Pai et al. 2014) as a
181 validation dataset. Additionally, we defined the onset and withdrawal dates of the rainy season
182 using the daily NOAA Climate Prediction Center (CPC) precipitation data set (Xie et al. 2007)
183 and compared them with IMERG.

184

2.2 Methodology

2.2.1 Onset and Retreat

This study uses a simple objective definition to identify the onset and cessation dates of the wet season over India which are determined by finding the minima and maxima of the cumulative rainfall anomaly curve (Liebmann and Marengo 2001). The cumulative anomaly of the daily rainfall at a day J (*i.e.,* $C_i(J)$) for a year i at each grid point is estimated as:

$$C_i(J) = \sum_{j=1}^{J}(R_i(j) - \bar{R}) \qquad (1)$$

where $R_i(j)$ is the rainfall for day j of year i, $\bar{R}$ is the climatology of the annual mean rainfall for a given grid point. The $C_i(J)$ for 365/366 days in a year represents the cumulative rainfall anomaly curve. After the onset and withdrawal dates of the season are determined, we count the number of days between them to define the seasonal length. Seasonal rainfall of the rainy season refers to the daily rainfall that accumulates from the day of onset date to the withdrawal date.

2.2.2 Perturbation

The motivation to perturb the timeseries is to account for the uncertainty of random synoptic or mesoscale events that is potentially unrelated to the seasonal cycle, which could affect the diagnosis of the onset/withdrawal date of the rainy season. The threat of false diagnosis of onset/withdrawal dates of the rainy season is acute from the proposed methodology since this diagnosis is computed at the granularity of the rainfall analysis. Therefore, generating an ensemble of onset/withdrawal dates of the rainy season that accounts for this uncertainty is essential. The perturbations are generated randomly by replacing the rainfall of each day in the original timeseries for a given grid point by rainfall in the range of $\pm$ 3 days. The range of $\pm$ 3 days used in the generation of the perturbed timeseries covers the uncertainty in the occurrence of the synoptic (1 to 7 days) to meso-scale (1 to 3 days) rain features of the rainy season. In this manner, an ensemble of 101 (100 perturbations + 1 original) timeseries are generated. The diagnosis of the onset/withdrawal date of the rainy season will converge or diverge amongst the ensemble members if it is found to be insensitive or sensitive to these random rain events, respectively.

2.2.3 Signal-to-noise Ratio

We estimated the signal-to-noise ratio of the four quantities by utilizing the 101 ensemble members.

218 $$S_{noise}^2 = \frac{1}{A(B-1)} \sum_{a=1}^{A} \sum_{b=1}^{B} (X_{ab} - \bar{X}_b)^2 \qquad (2)$$

219 $$S_{signal}^2 = S_{em}^2 - \frac{1}{b} S_{noise}^2 \qquad (3)$$

220 Where, X belongs to any of the four quantities such as onset date, withdrawal date, seasonal length,

221 and seasonal rainfall anomalies of the varying rainy season, a and b are indices for A years and B

222 ensemble members, respectively. S_{em}^2 represents the measured total signal variance in the data over

223 A years and which is defined as;

224 $$S_{em}^2 = \frac{1}{(A-1)} \sum_{a=1}^{A} (\bar{X}_a - \bar{\bar{X}})^2,$$

225 And $\bar{X}_a = \frac{1}{(B-1)} \sum_{b=1}^{B} X_{ab}$, $\bar{\bar{X}} = \frac{1}{(A-1)} \sum_{a=1}^{A} \bar{X}_a$,

226 The signal-to-noise ratio is then given by:

227 $$ratio = \frac{S_{signal}^2}{S_{noise}^2} \qquad (4)$$

228 When $ratio < 1$ then it indicates that noise (or chaotic variations) is dominant, and the signal

229 dominates when $ratio > 1$. A strong signal indicates that perturbing the rainfall time series will

230 not substantially influence the diagnostics of the onset date, withdrawal date, seasonal length, and

231 seasonal rainfall anomalies.

232

233 **2.2.4 Significance test**

234 In this study, we first estimate the two-tailed p-values of the correlation coefficients using the t-

235 statistic. Further, following Benjamini and Hochberg (1995), we conduct a test for false rejection

236 on all temporal correlations to assess its robustness, which is necessary because of the large number

237 of simultaneous statistical significance tests conducted across all grid points of the domain. This

238 process involves adjusting the p-value (Benjamini and Hochberg 1995) to control the false

239 rejection of the null hypothesis, also known as the false discovery rate. By controlling the false

240 discovery rate, we enhance the confidence in the significance of the findings.

241

242 **3. Results**

243   The seasonal mean rainfall over India observed from IMERG is found to be comparable with IMD
244   observation and superior to other satellite products over the region (Saikrishna et al., 2021). This
245   is further confirmed in Figs. 1a-c which compares the 23-year annual mean rainfall climatology
246   between IMERG observations and the corresponding IMD rainfall dataset. It may be noted that in
247   Equation (1), the annual mean rainfall climatology ($\bar{R}$) at each grid point is used to determine
248   onset dates and withdrawal dates of the rainy season over India (e.g., Misra et al., 2018). Overall,
249   the annual mean rainfall climatology from IMERG compares well with the IMD rain gauge dataset.
250   However, the overestimation of rainfall in the Indo-Gangetic plains and parts of northeast India
251   and underestimation of rainfall over the northern Western Ghats, northern sections of northeast
252   India, and the bulk of Jammu and Kashmir by IMERG relative to IMD dataset is apparent (Fig. 1).
253   Bushair et al., (2019) noted that IMERG underestimates the rainfall over high-altitude regions
254   compared to IMD observations, which are rain gauge based. Further, Fig. 1d shows the cumulative
255   rainfall anomaly curve generated from the 23-year (2001 - 2023) daily rainfall climatology area
256   averaged over all of India for IMERG (blue) and IMD (red) observations. The onset (inflection at
257   the nadir of the cumulative anomaly curve) and withdrawal (inflection at the zenith of the
258   cumulative anomaly curve) dates estimated from IMERG and IMD closely match each other, with
259   the onset dates being 31st May and 3rd June, and the withdrawal dates being 7th October and 8th
260   October, respectively.
261

262
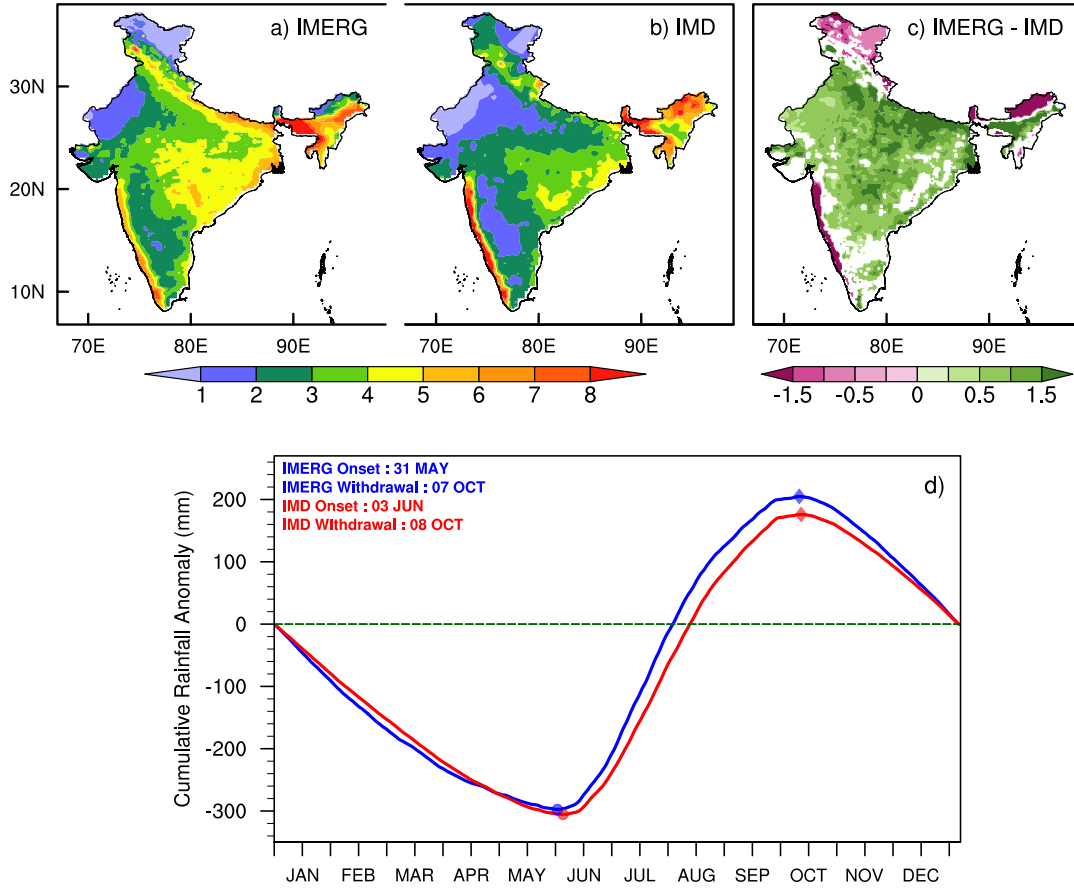
Figure 1: *Spatial pattern of the 23-year climatology of the mean annual rainfall (mm/day) during the period 2001-2023 from a) IMERG observation, b) IMD observation, and c) the difference between the IMERG and IMD (only differences significant at 5% percentile level on t-test is shaded). d) The cumulative rainfall anomaly curve generated from the 23-year daily rainfall climatology of IMERG (blue) and IMD (red) observations. The onset dates (filled circles) and withdrawal dates (filled diamonds) obtained from both datasets are marked.*

Figures 2a-d depict the 23-year local climatological onset date, withdrawal date, seasonal length, and seasonal accumulated rainfall from IMERG, with the associated standard deviation displayed in Figs. 2e-h. The spatial distribution of the climatology of the onset dates (Fig. 2a) shows the earliest onset occurs over northeast regions of India followed by southern Kerala, and then it gradually advances to the other parts of the country and looks like the typical isochrone evolution of the ISM (Ramage 1971; Rao 1976; Janowiak and Xie 2003). The delayed onset occurs over the east coast of Tamil Nadu followed by Jammu and Kashmir. The onset dates over Kerala and

277 adjacent regions mostly start from early May and do not coincide with the MoK, and this is because
278 this methodology detects the onset dates relatively early due to strong and continuous spells of
279 pre-monsoon rainfall. Similarly, the earliest withdrawal (Fig. 2b) of the ISM occurs over
280 northwestern India such as Rajasthan, Punjab, Haryana, and Himachal Pradesh. The withdrawal
281 date is delayed over southern peninsular India, with the most delayed withdrawal occurring over
282 the southeast coast of Tamil Nadu. The seasonal length (Fig. 2c) is shorter in the west and
283 northwest regions of India, with the shortest season in Jammu and Kashmir. The longer season
284 over the peninsular India, as well as the coastal regions of Odisha and West Bengal, is linked to
285 the season's earlier start date. The spatial distribution of the seasonal accumulated rainfall (Fig.
286 2d) closely follows the typical seasonal mean ISM distribution. The standard deviation patterns of
287 the onset dates show central parts of India have less variability than other regions, such as southern
288 peninsular India, northeast, and northwest regions. Similar patterns of variability are observed in
289 the withdrawal dates and seasonal length with the largest variations found over southern peninsular
290 India and northwest India and least over central India. On the other hand, the seasonal rainfall
291 exhibits a significant range of variability across most of India, whereas comparatively less
292 variability is observed over Rajasthan and Jammu and Kashmir.

293
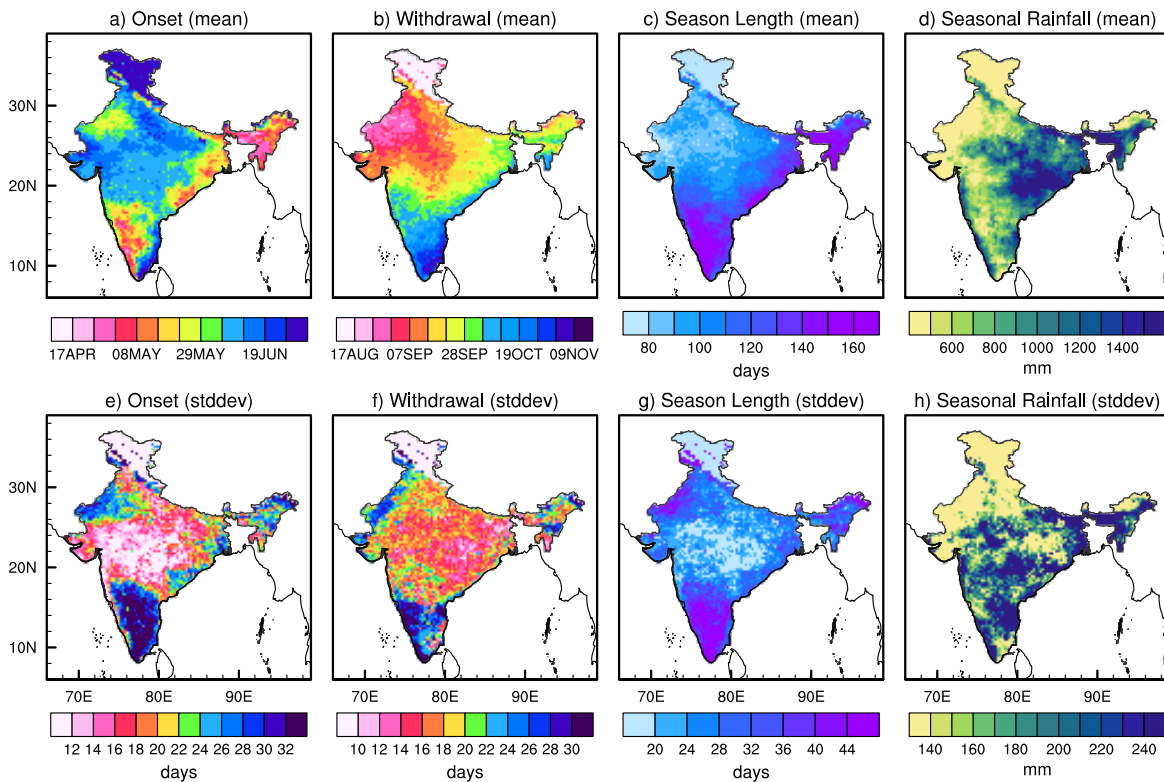
***Figure 2**: The climatological a) onset date (Julian day), b) withdrawal date (Julian day), c) seasonal length, and d) seasonal accumulated rainfall (mm) of the rainy season from IMERG. The corresponding standard deviation of e) onset date (days), f) withdrawal date (days), g) seasonal length (days), and h) seasonal accumulated rainfall (mm). The contour intervals in panels (a) and (b) are at 7-day interval.*

The IMERG dataset, with its 23-year record, was compared to the IMD and CPC datasets spanning 1979–2023 (limited to this period in order for CPC and IMD to have a common period) to evaluate onset and withdrawal dates, seasonal length, and seasonal accumulated rainfall of the rainy season over India (Fig. S2). The motivation to carry out this comparison is to establish that a 23-year record of IMERG is comparable to a longer record of dataset available from the other two sources besides examining its fidelity.

It is apparent from Fig. S2 that the spatial patterns of the climatological onset and withdrawal dates, seasonal length, and rainfall in IMERG is comparable to corresponding climatologies from IMD and CPC datasets. There is however a tendency for IMERG to have a bias of a slightly earlier onset of the rainy season compared to IMD and CPC, particularly over southern peninsular India, including Kerala and Tamil Nadu (Figs. S2a-c). Similar inference can be drawn in Rajasthan, coastal Odisha and West Bengal, and few isolated grid points over other regions. In contrast, over Jammu and Kashmir, IMERG exhibits a noticeably delayed onset, which makes us unsure about the results over this area. Similarly, IMERG display a systematic bias of slightly later withdrawal dates along the Western Ghats, but overall, the rainy season withdrawal dates are consistent across datasets (Figs. S2e-g). As a result, IMERG's rainy season seems to last longer than the other two datasets in some of these locations (Figs. S2i-k). Again, in terms of seasonal accumulated rainfall (Figs. S2m-o), IMERG overestimates precipitation compared to IMD and CPC in some of these locations. However, rainfall over the Western Ghats exhibits stronger gradients and is underestimated in IMERG while it exhibits more rainfall over western central India and Tamil Nadu than the other two datasets.

The interannual variability of these variables in IMERG also appear to be comparable to the other two datasets, especially in their spatial gradients (Fig. S3). There are however instances of some

325 differences in the datasets. For example, over central India, the standard deviation of seasonal
326 rainfall is significantly overestimated in IMERG compared to IMD (Figs. S3m-o), even though
327 the withdrawal dates (Figs. S3e-g) and seasonal length (Figs. S3i-k) exhibit less variability in
328 IMERG.

330 As mentioned earlier, IMERG has few different rainfall products based on the latency of their
331 availability in real-time. We have made comparisons of 12-hour latency product with the Final
332 product of IMERG in Figs. S1, S2, and S3. The comparison in Fig. S1 indicates that some of the
333 largest differences in the seasonal rain of the variable rainy season between Final and 12-hour
334 latency of IMERG is over northern India. However, the spatial patterns of the climatological onset
335 appear comparable (Figs. S2c and d). But the climatological withdrawal dates appear to be slightly
336 earlier in northern India in the Final run (Fig. S2h) compared to 12-hour latency (Fig. S2g) of
337 IMERG, which likely leads to slightly shorter length (Fig. S2l) and reduced seasonal rainfall (Fig.
338 S2p) in the former (Fig. S2l) than in the latter (Figs. S2k and o). Some of the discrepancies
339 observed in the 12 hour latency product of IMERG relative to IMD and CPC in Figs. S2 and S3
340 can likely be attributed to the uncertainty associated with the choice of the 12-hour latency product,
341 which is an early version of IMERG with limited calibration against ground-based observations,
342 its shorter temporal coverage of 23 years compared to the 45 years of data used for IMD and CPC.
343 Despite these limitations, which seem to be tolerable for the applications of this study (compare
344 Fig. 1) we are inclined to use IMERG due to its higher spatial resolution and near real-time
345 availability making it particularly suitable for real-time applications.

347 The primary motivation to monitor the local onset and withdrawal of the ISM is its significant
348 interannual variations and spatial variability (Fig. S3). Both the variation in seasonal length and
349 seasonal rainfall are crucial in determining the nature of the rainy season (Xavier et al.
350 2007; Sperber and Annamalai 2014). The spatial distribution of the correlation of the local onset
351 date with the seasonal length shows a significant negative correlation across India except in some
352 parts of central India and Jammu and Kashmir (Fig. 3a). This negative correlation suggests that an
353 early or later onset date is likely to be associated with a longer or a shorter rainy season,
354 respectively. Only the correlations significant at a 5% level are shaded (non-significant values are
355 shown in white) in Fig. 3. Similarly, early onset is associated with a wetter season, while a delayed

356   onset is linked with a drier season (Fig. 3b). However, the grid points showing significant

357   correlation are fewer in Fig. 3b compared to Fig. 3a. The correlations of the withdrawal date with

358   seasonal length (Fig. 3c) and seasonal rainfall anomalies (Fig. 3d) show that later or early

359   withdrawal of the wet season corresponds to a longer and wetter season, whereas an earlier

360   withdrawal corresponds to shorter and drier seasons. While the correlation between seasonal

361   rainfall and onset/withdrawal dates appears weaker than that with seasonal length, over 50% of

362   grid points across India still show statistically significant relationships. This is expected, as total

363   rainfall during the rainy season is influenced by variations in the seasonal length but also daily rain

364   rate, which can be influenced by various factors like tropical cyclones and intraseasonal weather

365   patterns that may lead to a weak correlation with onset/withdrawal dates. However, the withdrawal

366   date may not be a useful predictor for the rainy season because it occurs when the rainy season

367   ends. The onset and withdrawal dates are largely uncorrelated (not shown), implying that their

368   variations are independent of each other. These outcomes imply that the onset date alone can be a

369   useful predictor for the outlook of the seasonal length and the seasonal rainfall anomaly of the

370   forthcoming rainy season.

371
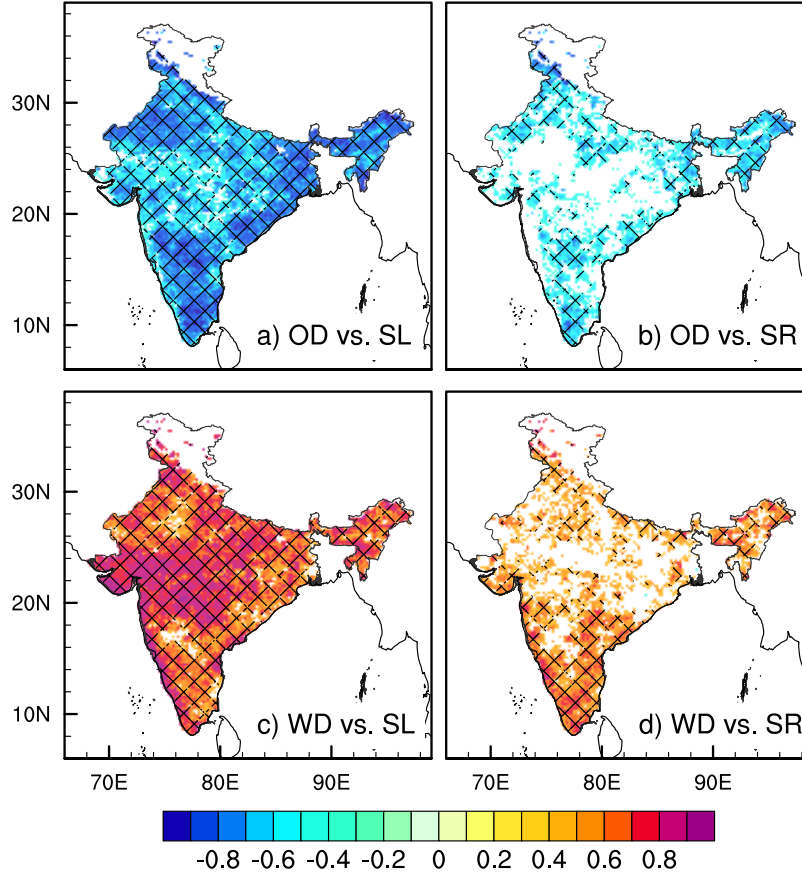
Figure 3: *The correlation coefficients of the onset date (OD) with a) seasonal length (SL), and b) seasonal rain (SR). Similarly, the correlations of withdrawal date (WD) with c) SL and d) SR. The shading indicates statistical significance at a 5% significance level according to the t-statistic (non-significant values are shown in white), following false discovery rate testing as described by Benjamini and Hochberg (1995). Cross hatchings denote correlations greater than or equal to +/- 0.6.*

We estimated the signal-to-noise ratio (Equation 4) on the four variables of onset and withdrawal dates, seasonal length, and rainfall by utilizing the 101-member ensemble of time-series data. This analysis examines the spread across ensemble members and informs on the uncertainty of the diagnosis to random rain events. The signal-to-noise ratio for onset dates (Fig. 4a) shows that noise dominates in many places, particularly in peninsular India and the eastern half of central India. These low signal-to-noise ratio regions suggests that onset dates of the rainy season are not very strongly tied to the seasonal cycle and predicting the onset dates in these places becomes challenging and less reliable. In contrast, the signal-to-noise ratios for withdrawal dates (Fig. 4b)

388 are typically more than one over most grid points. This indicates greater certainty for withdrawal

389 dates, particularly in areas like Kerala, coastal Karnataka, and Gujarat, where the ratios are

390 comparatively higher than one. In the case of the seasonal length, signal dominates over noise with

391 a signal-to-noise ratio above 1 over most areas (Fig. 4c). Compared to the other variables, seasonal

392 rainfall generally shows much higher signal-to-noise ratios (> 1) across most of the grid points.

393 This result is obvious given the fact that seasonal rainfall is an aggregate of the daily rainfall over

394 the entire rainy season, while the onset and withdrawal dates are single days of the season when

395 they are diagnosed. Therefore, there is a tendency for the cancellation of the noise in the

396 aggregation of the daily rainfall to seasonal rainfall, which yields a higher signal-to-noise ratio.

397
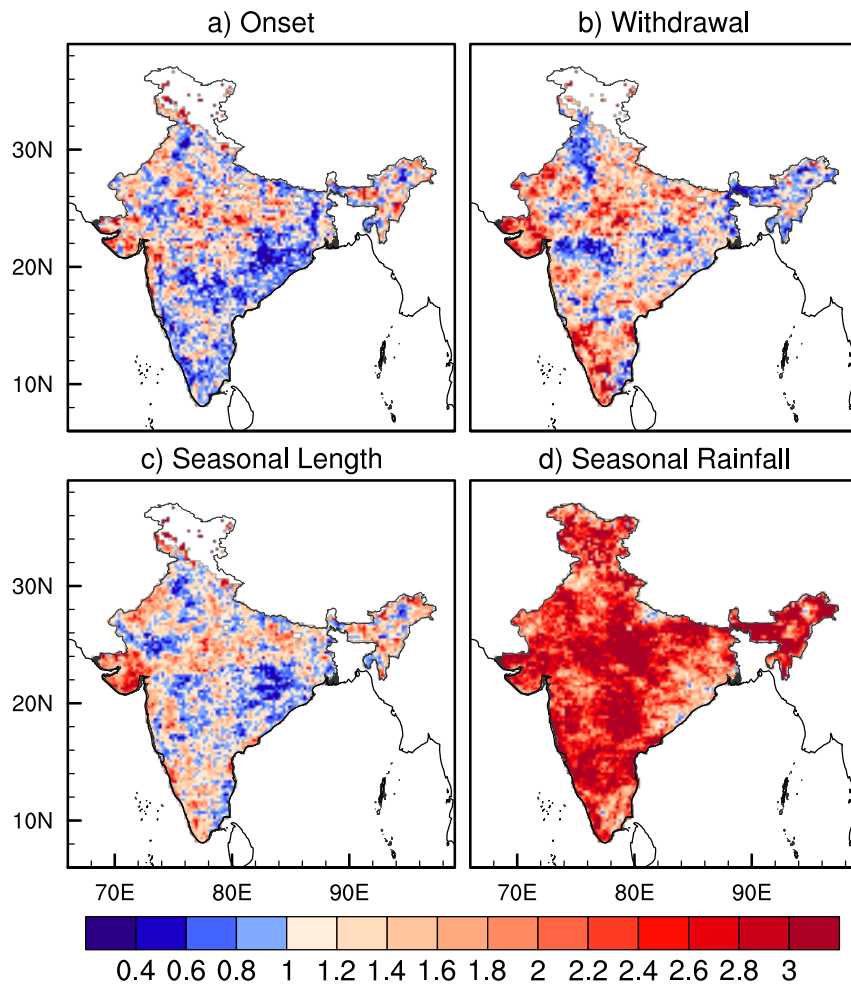
398 ***Figure 4****: The 23-year climatology of the signal-to-noise ratio of a) onset date, b) withdrawal date,*

399 *c) seasonal length, and d) seasonal rainfall estimated based on the 101 ensemble members.*

Further, we examined the probabilistic skill of the seasonal outlook by using the Area Under the relative operating characteristic (ROC) Curve (AUC) method. The AUC method is widely used to assess the skill of seasonal climate predictions (Mason and Graham 2002; Misra 2004; Narotsky and Misra 2021). Previous studies have shown that this method is useful for evaluating the probabilistic skill of predicting anomalous seasons based on anomalous onset dates of the rainy season (e.g. Rodgers et al 2024). We categorized the onset date, seasonal length, and seasonal rainfall into terciles (23-years divided into three groups): the lower tercile represents an early onset, shorter season, and drier conditions; the upper tercile signifies a delayed onset, longer season, and wetter conditions; and the middle tercile indicates normal onset, length, and seasonal rainfall. We then created a contingency table (Table S1) to assess the probability of categorical forecasts. This table evaluates how often an early or late onset is linked with a shorter or longer season and with drier or wetter conditions, respectively. In addition, we also consider the effects of normal onset on normal length and seasonal rainfall.
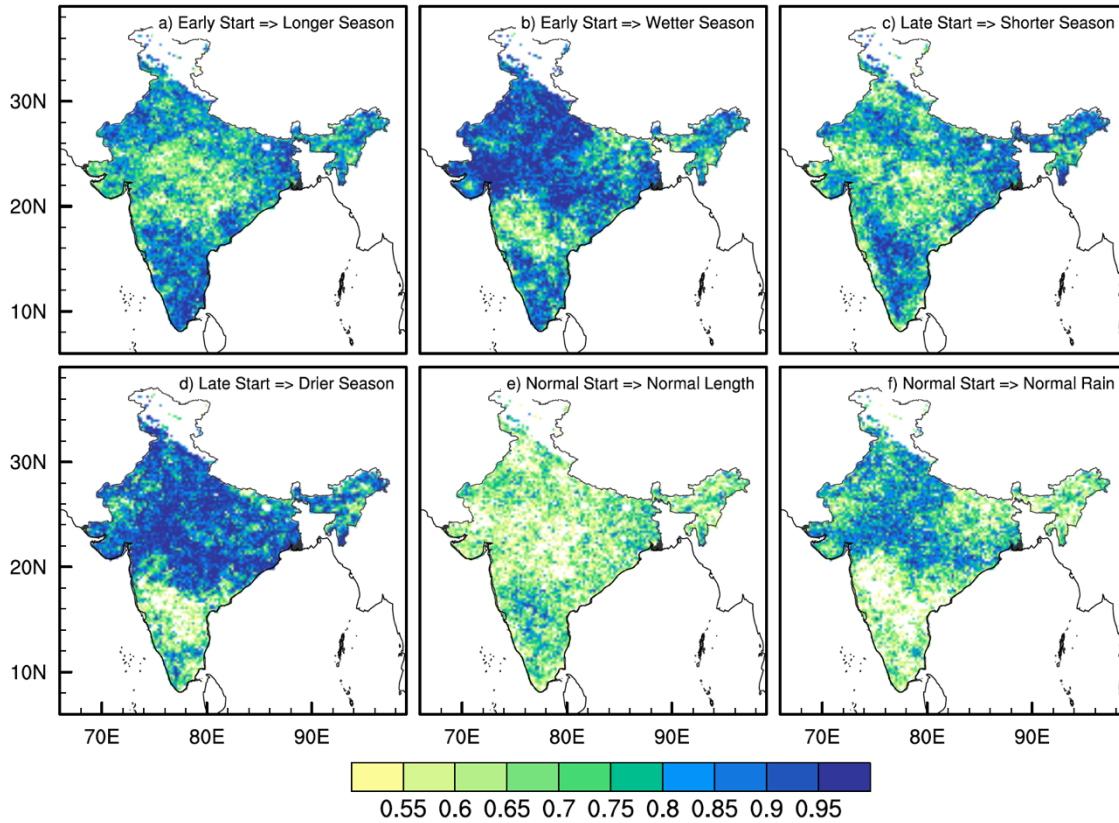
Figure 5: *The probabilistic skill score as measured by the Area Under the relative operating characteristic Curve (AUC) for early start (lowest tercile) season associated with a) longer*

(highest tercile) and b) wetter (highest tercile) season, late start (highest tercile) season associated

with c) shorter (lowest tercile) and d) drier (lowest tercile) season, and normal (middle tercile)

start season associated with e) normal (middle tercile) seasonal length and f) normal (middle

tercile) seasonal rain. The AUC above 0.5 is shaded.

The probabilistic skill scores derived from the AUC method are shown in Fig. 5. Here, only grid points with AUC values ≥ 0.5 are shaded, as these points indicate skillful seasonal outlooks that outperform random predictions (Mason and Graham, 2002). The seasons with an early start and longer season (Fig. 5a) show the most skill (>0.9) over peninsular India, northwest India, and some parts of northeast India. Similarly, the early start of the season, along with the wetter season (Fig. 5b), results in high skill levels across most parts of India except the majority of Maharashtra and north interior Karnataka. The late start and associated shorter seasons shown in Fig. 5c exhibit the highest skill score over some parts of peninsular India. The late start with the drier season also resulted in high skill scores across most of the areas except Kerala, Tamil Nadu, Karnataka and Andhra Pradesh. The anomalous seasons (Fig. 5a-d) demonstrate higher skill levels across India compared to the normal seasons (Fig. 5e-f). This is due to the leveraging of the linear relationships of the onset date variations with the rainy season variations (Figs. 3a and b). In contrast, seasons with a normal start of the rainy season exhibit lower AUC skill scores (Figs. 5e and f) across most grid points relative to the anomalous start of the rainy seasons (Figs. 5a-d). However, the skill scores for a normal start with normal rainfall (Fig. 5f) are slightly better than those for a normal start with normal length (Fig. 5e). In summary, the behavior of the forthcoming season is more predictable if the onset date is early or delayed than the normal. It is easy to adopt this methodology for real-time applications. The evolution of the daily cumulative anomaly curve of rainfall could be monitored in real-time to find the minima in the curve as the onset date. However, to avoid misdiagnosing the onset date of the rainy season, one could wait for a period of time after this diagnosis (typically a week) to confirm that the minima were indeed reached to declare the onset date. Once the onset date is diagnosed then one could use the linear relationships shown in Fig. 3 to develop a seasonal outlook for the rainy season. This is done routinely in Florida (Misra et al. 2022). With the availability of the merged IMERG estimates with the rain-gauge based IMD rainfall following Mitra et al., (2009) our proposed methodology could be adopted for real-time applications over India.

447

448   Further, we investigated the interannual variability of the onset dates over India and its association

449   with ENSO (Figure S4) and the Indian Ocean Dipole (IOD) variations (Figure S5). In comparison

450   to Figure 3, Figures S4 and S5 failed the BH test suggesting the lack of robustness in the

451   teleconnections of the rainy season variations with either ENSO or IOD. It should be noted that

452   the results in Figures S4 and S5 appear to be contrary to many other studies that suggest a robust

453   teleconnection of ENSO with ISM (e. g., Webster et al. 1998, Delsole and Shukla 2002). However,

454   our variable definition of the rainy season, which includes pre- and post-monsoon rainfall, would

455   make the comparison with other studies dealing with fixed calendar ISM season and or all India

456   averaged rainfall of the ISM incompatible. But in light of these results, which indicate a lack of

457   strong external forcing, the significance of the reliability of the seasonal outlook of the rainy season

458   shown in Figure 5 assumes greater significance. Furthermore, the monitoring of the observations

459   of the evolution of the rainy season, to diagnose the onset dates seems an attractive approach with

460   the relatively low signal-to-noise ratio of the onset date of the rainy season shown in Figure 4a,

461   relative to the seasonal length in Figure 4c or seasonal rainfall in Figure 4d. We are then able to

462   leverage a low signal-to-noise ratio quantity like the onset date of the rainy season to provide a

463   seasonal outlook of relatively higher signal-to-noise ratio quantities of seasonal length and rainfall.

464

465   **4. Summary and Concluding Remarks**

466   The seasonal prediction of the Indian rainy season is a considerable challenge given its complex

467   spatio-temporal variations. In this study, we offer a simple and reliable technique for seasonal

468   outlook of the rainy season, which is viable for real-time applications as well. Using precipitation

469   estimates of IMERG version 6 over India at 10km grid, we generate an ensemble of 101 members

470   from randomly perturbing the series to assess the uncertainty of the diagnosed onset/withdrawal

471   dates of the rainy season to random synoptic-meso scale rain events unconnected to the seasonal

472   cycle. The proposed method generates a spatial distribution of local-scale onset and withdrawal

473   dates, capturing regional variations and offering a nuanced view of progression rainy season across

474   India. Such location-specific information is useful for practical applications such as agriculture,

475   disaster planning, and water management.

476

477   We verified the IMERG rainfall observations against gauge-based IMD observations. The mean
478   annual rainfall climatology of IMERG closely matches that of the IMD. However, IMERG tends
479   to underestimate mean annual rainfall in high-altitude regions and overestimate it in the Indo-
480   Gangetic plains. Further, we examined the relationships between the onset and withdrawal dates
481   with seasonal length and rainfall and discovered that variations in onset and withdrawal dates of
482   the rainy season across India have a significant impact on the seasonal length and the seasonal
483   rainfall variations of the rainy season. It is found that an earlier onset date of the rainy season is
484   strongly related to a longer and wetter season, whereas a later onset date corresponds to a shorter
485   and drier season. However, the relationship between the onset, withdrawal, seasonal length, and
486   rainfall with large-scale climate drivers such as ENSO and IOD is comparatively weaker in major
487   parts of India. Although the influence of ENSO and IOD were investigated in this study, future
488   research could investigate the influence of additional teleconnection patterns such as the Madden–
489   Julian Oscillation (MJO), Pacific Decadal Oscillation (PDO), and North Atlantic Oscillation
490   (NAO), which may also modulate the timing and characteristics of the rainy season.

491

492   This study shows that by estimating the onset date of the rainy season alone we can effectively
493   provide a reliable seasonal outlook for both the seasonal length and total rainfall of the upcoming
494   season by exploiting the existing local relationships. The low signal to noise ratio of the onset date
495   of the rainy season suggests the dominance of internal variations, which will be a challenge for its
496   seasonal predictability. However, by way of monitoring the evolution of the onset date we can
497   leverage its local relationship with the seasonal length and seasonal rainfall anomaly to provide
498   reliable seasonal outlook of the rainy season. The probabilistic skill scores of these seasonal
499   outlooks generated from the monitoring of the onset date variations present an objective measure
500   of its high confidence of reliability. Compared to traditional ISM onset definitions, which often
501   focus on Kerala (e.g., MoK), the proposed method can generate spatial maps of local-scale onset
502   dates of the rainy season. It captures regional heterogeneity and the progression of the rainy season
503   across India. Since the method is based on the rainy season and includes pre- and post-monsoon
504   rainfall, it provides a comprehensive viewpoint of the rainy season. These seasonal outlooks have
505   numerous potential applications, and many local communities could greatly benefit from them.
506   The proposed methodology for the seasonal outlook of the rainy season over India demonstrates

507 its adaptation for real-time applications from the current availability of IMERG rainfall products

508 in real-time.

509

510 **Acknowledgments**

511 We acknowledge the support from NASA grant 80NSSC22K0595.

512

513 **Code/Data Availability**

514 The IMERG rainfall dataset is available from the NASA GES DISC

515 (https://gpm1.gesdisc.eosdis.nasa.gov/data/GPM_L3/GPM_3IMERGDL.06/). The India

516 Meteorological Department rainfall data set used for the analysis in this study is available at

517 https://www.imdpune.gov.in/cmpg/Griddata/Rainfall_25_NetCDF.html. The daily CPC data is

518 obtained from https://psl.noaa.gov/data/gridded/data.cpc.globalprecip.html. The Python and NCL

519 codes used for the analysis can be provided by the corresponding authors upon request.

520

521 **Author contribution**

522 The study was conceptualized by CBJ and VM. CBJ carried out the analysis and validation and

523 prepared the original manuscript. VM supervised the work, acquired funding, and reviewed and

524 edited the manuscript.

525

526 **Competing interests**

527 The authors declare that they have no conflict of interest.

528

529 **Reference:**

530 1. Ananthakrishnan, R., and M. K. Soman, (1988). The onset of the southwest monsoon over

531   Kerala: 1901–1980. J. Climatol., **8**, 283–296, doi:10.1002/joc.3370080305.

532 2. Bansod, S. D., S. V. Singh, and R. H. Kripalani, 1991: The relationship of monsoon onset

533   with subsequent rainfall over India. *Int. J. Climatol.*, **11**, 809–817,

534   doi:10.1002/joc.3370110707.

535 3. Benjamini, Y., & Hochberg, Y. (1995). Controlling the false discovery rate: A practical and

536   powerful approach to multiple testing. Journal of the Royal Statistical Society: Series

537   B, 57(1), 289–300. https://doi.org/10.1111/j.2517-6161.1995.tb02031.x

538 4. Bhardwaj, A., & Misra, V. (2019). Monitoring the Indian summer monsoon evolution at
539   the granularity of the Indian meteorological sub-divisions using remotely sensed rainfall
540   products. Remote Sensing, 11(9), 1080. https://doi.org/10.3390/rs11091080

541 5. Bombardi, R. J., Moron, V., & Goodnight, J. S. (2020). Detection, variability, and
542   predictability of monsoon onset and withdrawal dates: A review. Int. J. Climatol, 40(2),
543   641-667. https://doi.org/10.1002/joc.6264

544 6. Bushair, M. T., Kumar, P., & Gairola, R. M. (2019). Evaluation and assimilation of various
545   satellite-derived rainfall products over India. International Journal of Remote Sensing, 1–
546   24. https://doi.org/10.1080/01431161.2019.1579389

547 7. Choudhury, D., Nath, D., & Chen, W. (2021). The modulation of Indian summer monsoon
548   onset processes during ENSO through equatorward migration of the subtropical jet
549   stream. Climate Dynamics, 57(1), 141-152. https://doi.org/10.1007/s00382-021-05700-4.

550 8. Delsole, T, and J. Shukla, (2002). Linear prediction of Indian Monsoon Rainfall. J. Climate,
551   15, 3645-3658. https://doi.org/10.1175/1520-0442(2002)015<3645;LPOIMR>2.0.CO;2

552 9. Dhar, O. N., P. R. Rakhecha, and B. N. Mandal (1980), Does the early or late onset of
553   monsoon provide any clue to subsequent rainfall during the monsoon season, Mon.
554   Weather Rev., 108, 1069–1072, doi:10.1175/1520-0493(1980)1082.0.CO;2

555 10. Fasullo J, Webster PJ (2003) A hydrological definition of Indian monsoon onset and
556   withdrawal. J Climate 16:3200–321. https://doi.org/10.1175/1520-
557   0442(2003)016<3200a:AHDOIM>2.0.CO;2

558 11. Fitzpatrick, R. G., Parker, D. J., & Willetts, P. D. (2016). Assessing the level of spatial
559   homogeneity of the agronomic Indian monsoon onset. Geophysical Research Letters,
560   43(22), 11-867. https://doi.org/10.1002/2016GL070711

561 12. Gadgil, S.; Gadgil, S (2006). The Indian Monsoon, GDP and Agriculture. Econ. Polit.
562   Wkly. 41, 4887–4895. https://www.jstor.org/stable/4418949

563 13. Goswami, B. N., & Mohan, R. A. (2001). Intraseasonal oscillations and interannual
564   variability of the Indian summer monsoon. Journal of climate, 14(6), 1180-1198.
565   https://doi.org/10.1175/1520-0442(2001)014<1180:IOAIVO>2.0.CO;2

566 14. Goswami, B. N., & Xavier, P. K. (2005). ENSO control on the south Asian monsoon
567   through the length of the rainy season. *Geophysical Research Letters*, *32*(18).
568   https://doi.org/10.1029/2005GL023216

569 15. Huffman, G. J., Bolvin, D. T., Braithwaite, D., Hsu, K. L., Joyce, R. J., Kidd, C., ... & Xie,
570   P. (2020). Integrated multi-satellite retrievals for the global precipitation measurement
571   (GPM) mission (IMERG). In *Satellite precipitation measurement: Volume 1* (pp. 343-353).
572   Cham: Springer International Publishing. https://doi.org/10.1007/978-3-030-24568-9_19

573 16. Janowiak, J. E., and P. Xie (2003), A global-scale examination of monsoon-related
574   precipitation, J. Clim., 16, 4121–4133. https://doi.org/10.1175/1520-
575   0442(2003)016<4121:AGEOMP>2.0.CO;2

576 17. Joseph PV, Eishcheid JK, Pyle RJ. (1994). Interannual variability of the onset of the Indian
577   summer monsoon and its association with atmospheric features, El Nino, and sea surface
578   temperature anomalies. Journal of Climate 7: 81–105. https://doi.org/10.1175/1520-
579   0442(1994)007<0081:IVOTOO>2.0.CO;2

580 18. Joseph PV, Sooraj KP, Rajan CK (2006). The summer monsoon onset process over South
581   Asia and an objective method for the date of monsoon onset over Kerala. Int J Climatol
582   26:1871–1893. https://doi.org/10.1002/joc.1340

583 19. Karmakar, N., & Misra, V. (2019). The relation of intraseasonal variations with local onset
584   and demise of the Indian summer monsoon. *Journal of Geophysical Research:*
585   *Atmospheres*, *124*(5), 2483-2506. https://doi.org/10.1029/2018JD029642

586 20. Khouakhi, A., Villarini, G., & Vecchi, G. A. (2017). Contribution of tropical cyclones to
587   rainfall at the global scale. Journal of Climate, 30(1), 359-372.
588   https://doi.org/10.1175/JCLI-D-16-0298.1

589 21. Kung, E. C., and Sharif, T. A., (1980). Regression forecasting of the onset of the India
590   summer monsoon with antecedent upper air conditions, J. Appl. Meteorol., V19, pp370—
591   380. https://doi.org/10.1175/1520-0450(1980)019<0370:RFOTOO>2.0.CO;2

592 22. Lal, M. (2000). Climatic change-implications for India's water resources. Journal of Social
593   and Economic Development, 3, 57-87. https://ideas.repec.org/a/sch/journl/v3y2001i1p57-
594   87.html

595 23. Liebmann, B., and J. Marengo, (2001). Interannual variability of the rainy season and
596   rainfall in the Brazilian Amazon basin. J. Climate, 14, 4308–4318,
597   https://doi.org/10.1175/1520-457 0442(2001) 014,4308:IVOTRS.2.0.CO;2.

598 24. Mason, S. J. and N. E. Graham, (2002). Areas beneath the relative operating characteristics
599   (ROC) and relative operating levels (ROL) curves: statistical significance and

interpretation. Quar. Roy. Soc., 128, 2145-2166. https://doi.org/10.1256/003590002320603584

25. Misra, V. (2004) An evaluation of the predictability of austral summer season precipitation over South America. Journal of Climate, **17**, 1161–1175. https://doi.org/10.1175/1520-0442(2004)017<1161:AEOTPO>2.0.CO;2

26. Misra, V., Dixit, S., & Jayasankar, C. B. (2023). The regional diagnosis of onset and demise of the rainy season over tropical and subtropical Australia. Earth Interactions, 27(1), 220026. https://doi.org/10.1175/EI-D-22-0026.1

27. Misra, V., Jayasankar, C. B., Beasley, P., & Bhardwaj, A. (2022). Operational monitoring of the evolution of rainy season over florida. Frontiers in Climate, 4, 793959. https://doi.org/10.3389/fclim.2022.793959

28. Misra, V.; Bhardwaj, A.; Mishra, A. (2018). Local onset and demise of the Indian summer monsoon. Clim. Dyn., 51, 1609–1622. https://doi.org/10.1007/s00382-017-3924-2

29. Misra, V.; Bhardwaj, A.; Noska, R. (2017) Understanding the Variations of the Length and the Seasonal Rainfall Anomalies of the Indian Summer Monsoon. J. Clim., 30, 1753–1763. https://doi.org/10.1175/JCLI-D-16-0501.1

30. Misra V, DiNapoli S (2014) The variability of the southeast Asian summer monsoon. Int J Climatol 34:893–901. https://doi.org/10.1002/joc.3735

31. Mitra, A. K., Bohra, A. K., Rajeevan, M. N., & Krishnamurti, T. N. (2009). Daily Indian precipitation analysis formed from a merge of rain-gauge data with the TRMM TMPA satellite-derived rainfall estimates. 87A, 265-279. https://doi.org/10.2151/jmsj.87A.265

32. Mooley, D. A., and B. Parthasarthy (1984), Fluctuations in all-India summer monsoon rainfall during 1871–1978, Clim. Change, 6(3), 287–301, doi:10.1007/BF00142477. https://doi.org/10.1007/BF00142477

33. Mooley, D. A., and J. Shukla (1987), Variability and forecasting of the summer monsoon rainfall over India, in Monsoon Meteorology, edited by C. P. Chang and T. N. Krishnamurti, pp. 26–59, Oxford Univ. Press, Oxford, U. K

34. Moron V, Robertson AW, (2014): Interannual variability of Indian summer monsoon rainfall onset date at local scale. Int J Climatol, 34(4). doi:10.1002/joc.3745

35. Noska, R.; Misra, V. (2016) Characterizing the onset and demise of the Indian summer monsoon. Geophys. Res. Lett., 43, 4547–4554. https://doi.org/10.1002/2016GL068409

631 36. Pai DS, Rajeevan M (2007) Indian Summer Monsoon Onset: variability and prediction.
632   NCC Research Report No. 6. National Climate Centre, Indian Meteorological Department.

633 37. Pai, D. S., & Rajeevan, M. N. (2009). Summer monsoon onset over Kerala: New definition
634   and prediction. Journal of Earth System Science, 118(2), 123-135.
635   https://doi.org/10.1007/s12040-009-0020-y

636 38. Pai, D. S., Rajeevan, M., Sreejith, O. P., Mukhopadhyay, B., & Satbha, N. S. (2014).
637   Development of a new high spatial resolution (0.25× 0.25) long period (1901-2010) daily
638   gridded rainfall data set over India and its comparison with existing data sets over the
639   region. Mausam, 65(1), 1-18. https://doi.org/10.54302/mausam.v65i1.851

640 39. Pai, D. S., Bandgar Arti, Devi Sunitha, Musale Madhuri, M. R. Badwaik, A. P. Kundale,
641   Gadgil Sulochana, M. Mohapatra, and M. Rajeevan. (2020) "Normal dates of
642   onset/progress and withdrawal of southwest monsoon over India." Mausam 71, no. 4, 553-
643   570. https://doi.org/10.54302/mausam.v71i4.33

644 40. Phadtare, J. A., Fletcher, J. K., Ross, A. N., Turner, A. G., Schiemann, R. K., & Burns, H.
645   L. (2023). Unravelling the mechanism of summer monsoon rainfall modes over the west
646   coast of India using model simulations. Quarterly Journal of the Royal Meteorological
647   Society, 149(757), 3164-3182. https://doi.org/10.1002/qj.4550

648 41. Pradhan, M., Rao, A. S., Srivastava, A., Dakate, A., Salunke, K., & Shameera, K. S. (2017).
649   Prediction of Indian summer-monsoon onset variability: A season in advance. Scientific
650   reports, 7(1), 14229. https://doi.org/10.1038/s41598-017-12594-y

651 42. Prasad, V. S. & Hayashi, T. Onset and withdrawal of Indian summer monsoon. Geophys.
652   Res. Lett. **32**, 1–5 (2005). https://doi.org/10.1029/2005GL023269

653 43. Preenu, P. N., Joseph, P. V., & Dineshkumar, P. K. (2017). Variability of the date of
654   monsoon onset over Kerala (India) of the period 1870–2014 and its relation to sea surface
655   temperature. Journal of Earth System Science, 126, 1-19. https://doi.org/10.1007/s12040-
656   017-0852-9

657 44. Rajeevan, M. and Dubey, D. P., (1995) Long range prediction of monsoon onset over
658   Kerala, Mausam, V46, pp287-290. https://doi.org/10.54302/mausam.v46i3.3261

659 45. Ramage, C. (1971), Monsoon Meteorology, Int. Geophys. Ser., vol. 15, 296 pp., Academic
660   Press, San Diego, Calif.

661   46. Ramesh Kumar, M. R., (2004) Forecasting of onset of southwest monsoon over Kerala
662   coast using satellite data, IEEE Geosci. Remote Sens. Lett., V1 (4), pp265-267.
663   10.1109/LGRS.2004.832226

664   47. Rao, Y. P. (1976) Southwest monsoon. Meteorological Monograph, Synoptic Meteorology,
665   367.

666   48. Rodgers, J., Misra, V., & Jayasankar, C. B. (2024). Using the observed variations of the
667   start date of the rainy season over Central America for its reliable seasonal outlook. Journal
668   of Climate. *37*(18), 4901–4913. https://doi.org/10.1175/JCLI-D-23-0699.1

669   49. Saikrishna, T. S., Ramu, D. A., & Osuri, K. K. (2021). Inter-comparison of high-resolution
670   satellite precipitation products over India during the summer monsoon
671   season. Meteorology and Atmospheric Physics, 133, 1675-1690.
672   https://doi.org/10.1007/s00703-021-00829-7

673   50. Sankar, S., Kumar, M. R., & Reason, C. (2011). On the relative roles of El Nino and Indian
674   Ocean Dipole events on the Monsoon Onset over Kerala. Theoretical and applied
675   climatology, 103, 359-374. https://doi.org/10.1007/s00704-010-0306-7

676   51. Sperber, K. R., and H. Annamalai, (2014) The use of fractional accumulated precipitation
677   for the evaluation of the annual cycle of monsoons. Climate Dyn., 43, 3219–3244,
678   doi:10.1007/s00382-014-2099-3.

679   52. Stolbova, V., Surovyatkina, E., Bookhagen, B., & Kurths, J. (2016). Tipping elements of
680   the Indian monsoon: Prediction of onset and withdrawal. Geophysical Research Letters,
681   43(8), 3982-3990. https://doi.org/10.1002/2016GL068392

682   53. Thakur, M. K., Kumar, T. L., Narayanan, M. S., Kundeti, K. R., & Barbosa, H. (2020).
683   Analytical study of the performance of the IMERG over the Indian
684   landmass. Meteorological Applications, 27(3), e1908. https://doi.org/10.1002/met.1908

685   54. Walker, J. M., & Bordoni, S. (2016). Onset and withdrawal of the large-scale South Asian
686   monsoon: A dynamical definition using change point detection. Geophysical Research
687   Letters, 43(22), 11-815. https://doi.org/10.1002/2016GL071026

688   55. Wang B, Ding Q, Joseph PV (2009) Objective definition of the Indian summer monsoon
689   onset. J Clim 22(12):3303–3316. https://doi.org/10.1175/2008JCLI2675.1

690   56. Wang B, LinHo (2002) Rainy season of the Asia-Pacific summer monsoon. J Climate
691   15:386–398. https://doi.org/10.1175/1520-0442(2002)015<0386:RSOTAP>2.0.CO;2

57. Wang, X., Jiang, X., Yang, S., & Li, Y. (2013). Different impacts of the two types of El Niño on Asian summer monsoon onset. Environmental Research Letters, 8(4), 575–591. DOI 10.1088/1748-9326/8/4/044053

58. Webster, P. J., V. O. Magana, T. N. Palmer, J. Shukla, R. A. Tomas, M. Yanai, and T. Yasunari, (1998) Monsoons: Processes, predictability, and the prospects for prediction. *J. Geophys. Res.*, **103** , 14451–14510. https://doi.org/10.1029/97JC02719

59. Xavier, P. K., C. Marzin, and B. N. Goswami, 2007: An objective definition of the Indian summer monsoon season and a new perspective on the ENSO–monsoon relationship. Quart. J. Roy. Meteor. Soc., 133, 749–764, doi:10.1002/qj.45.

60. Xie, P., A. Yatagai, M. Chen, T. Hayasaka, Y. Fukushima, C. Liu, and S. Yang (2007), A gauge-based analysis of daily precipitation over East Asia, J. Hydrometeorol., 8, 607. 626. https://doi.org/10.1175/JHM583.1

61. Zeng X, Lu E (2004) Globally unified monsoon onset and retreat indexes. J Climate 17:2241–2248. https://doi.org/10.1175/1520-0442(2004)017<2241:GUMOAR>2.0.CO;2